From March 2007 *High Frequency Electronics*

Spatially Selective Antenna for Very Close Proximity HF RFID Applications—Part 2

By Boris Y. Tsirline, PhD
Zebra Technologies Corporation

Part 2 of this article concludes the author's description and analysis of RFID antennas that are capable of communicating with a single transponder (tags) while in close proximity to other tags

This article continues the description and analysis of a novel HF antenna with high spatial selectivity. Its performance and functional characteristics are analyzed for two orthogonal alignments of the antenna and the trans-ponder using a simplified mathematical model.

Part 1 provided background on RFID technology, identified the problem to be solved, and began a discussion of the interaction of the antenna and the transponder. Part 2 continues the discussion, presenting an analysis of coupling mechanism between antenna and transponder with respect to their orientation and relative movement.

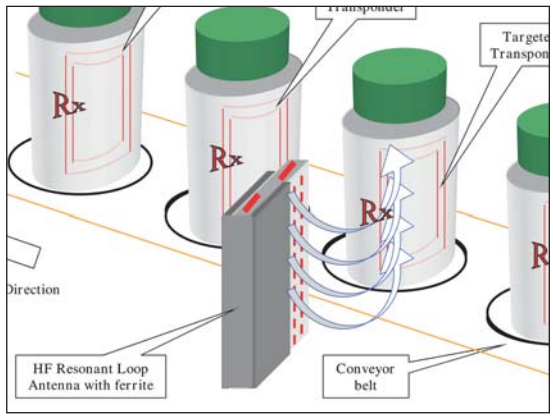

Figure 1 (detail) · HF antenna for item-level RFID on conveyer.

Magnetic Flux through Transponder

One possible way to overcome multi-interval interaction of an antenna-transponder and improve antenna performance is to use a finite conductive element (or elements grouped together) for the magnetic flux generation. The element can be a short straight wire carrying the time varying current. With the aim of achieving high spatial selectivity (SS), a straight short wire type HF antenna was proposed and implemented [9] for the smart label encoding process in RFID Printer-Encoders. This antenna is based on the conventional resonant rectangular loop antenna fabricated on PCB, where the traces provide the antenna conductors. Three sides of an antenna are covered by a flexible ferrite patch and one side is left open (Fig. 1). The ferrite patch amplifies the magnetic flux generated by the antenna and also concentrates the magnetic flux, increasing the coil inductance and it's Q-factor.

To analyze the performance of this original antenna design and estimate its SS, a mathematical model was developed. This model, by establishing a relationship between mechanical and electrical characteristics of an antenna-transponder structure, enables a comparison of the parameters for two orthogonal alignments.

As was declared above, Magnetic Flux through Transponder Φ_T is the most powerful parameter used for an antenna-transponder quality and performance characterization. It can be found using Equation (9). In the general case, this formula includes a spatial distribution of the non-uniform magnetic flux density generated by a current through a finite length rod, with a diameter much smaller then an antenna-transponder separation distance.

The the magnetic flux density at any field point normal to a transponder plane is produced by a short wire of length *2L* carrying a current *I* along the *(-x)* direction (Fig. 4) in accordance with Biot-Savart Law, which is written for a general case [10] as

$$Cos\theta = \frac{y}{\sqrt{y^2 + z_0^{\,2}}} \qquad (14)$$

The equation (14) includes a normalization of a vector **B** to the transponder plane by accepting an angle θ

$$Cos\theta = \frac{y}{\sqrt{y^2 + z_0^{\,2}}}$$

Integration area of the transponder (Fig. 4) is limited by its width ΔW and length ΔR. The total MFT Φ_T (9) for the interval $Y \geq 0$ can be obtained then by summing over the contributions from all transponder area differential elements $dA = dxdy$. This is eq. (15)

$$\Phi_T = \frac{\mu_0 NI}{4\pi} \int_R^{R+\Delta R} \frac{rdr}{\left(y^2 + z_0^{\,2}\right)} \int_W^{W+\Delta W} \frac{(x+L)\,dx}{\sqrt{(x+L)^2 + \left(y^2 + z_0^{\,2}\right)}} - \int_R^{R+\Delta R} \frac{rdr}{\left(y^2 + z_0^{\,2}\right)} \int_W^{W+\Delta W} \frac{(x+L)\,dx}{\sqrt{(x-L)^2 + \left(y^2 + z_0^{\,2}\right)}}$$

Carrying out the integration (see Appendix) gives eq. (16), shown below:

$$\begin{aligned}
\Phi_T = \frac{\mu_0 NI}{4\pi}\Bigg\{ & \sqrt{(R+\Delta R)^2 + z_0^{\,2} + (W+\Delta W+L)^2} - \sqrt{(R)^2 + z_0^{\,2} + (W+\Delta W+L)^2} - \\
& - \frac{(W+\Delta W+L)}{2} Ln \left| \frac{(W+\Delta W+L) + \sqrt{(R+\Delta R)^2 + z_0^{\,2} + (W+\Delta W+L)^2}}{(W+\Delta W+L) - \sqrt{(R+\Delta R)^2 + z_0^{\,2} + (W+\Delta W+L)^2}} \right| + \\
& + \frac{(W+\Delta W+L)}{2} Ln \left| \frac{(W+\Delta W+L) + \sqrt{R^2 + z_0^{\,2} + (W+\Delta W+L)^2}}{(W+\Delta W+L) - \sqrt{R^2 + z_0^{\,2} + (W+\Delta W+L)^2}} \right| - \\
& - \sqrt{(R+\Delta R)^2 + z_0^{\,2} + (W+L)^2} + \sqrt{(R)^2 + z_0^{\,2} + (W+L)^2} + \\
& + \frac{(W+L)}{2} Ln \left| \frac{(W+L) + \sqrt{(R+\Delta R)^2 + z_0^{\,2} + (W+L)^2}}{(W+L) - \sqrt{(R+\Delta R)^2 + z_0^{\,2} + (W+L)^2}} \right| - \\
& - \frac{(W+L)}{2} Ln \left| \frac{(W+L) + \sqrt{R^2 + z_0^{\,2} + (W+L)^2}}{(W+L) - \sqrt{R^2 + z_0^{\,2} + (W+L)^2}} \right| - \\
& - \sqrt{(R+\Delta R)^2 + z_0^{\,2} + (W+\Delta W-L)^2} + \sqrt{(R)^2 + z_0^{\,2} + (W+\Delta W-L)^2} + \\
& + \frac{(W+\Delta W-L)}{2} Ln \left| \frac{(W+\Delta W-L) + \sqrt{(R+\Delta R)^2 + z_0^{\,2} + (W+\Delta W-L)^2}}{(W+\Delta W-L) - \sqrt{(R+\Delta R)^2 + z_0^{\,2} + (W+\Delta W-L)^2}} \right| - \\
& - \frac{(W+\Delta W-L)}{2} Ln \left| \frac{(W+\Delta W-L) + \sqrt{R^2 + z_0^{\,2} + (W+\Delta W-L)^2}}{(W+\Delta W-L) - \sqrt{R^2 + z_0^{\,2} + (W+\Delta W-L)^2}} \right| + \\
& + \sqrt{(R+\Delta R)^2 + z_0^{\,2} + (W-L)^2} + \sqrt{(R)^2 + z_0^{\,2} + (W-L)^2} - \\
& - \frac{(W-L)}{2} Ln \left| \frac{(W-L) + \sqrt{(R+\Delta R)^2 + z_0^{\,2} + (W-L)^2}}{(W-L) - \sqrt{(R+\Delta R)^2 + z_0^{\,2} + (W-L)^2}} \right| + \\
& + \frac{(W-L)}{2} Ln \left| \frac{(W-L) + \sqrt{R^2 + z_0^{\,2} + (W-L)^2}}{(W+L) - \sqrt{R^2 + z_0^{\,2} + (W-L)^2}} \right| \Bigg\}
\end{aligned} \qquad \text{Eq. (16)}$$

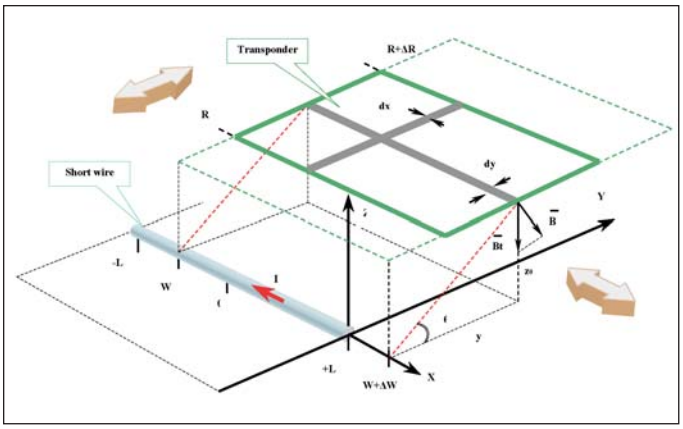

Figure 4 · Diagram showing the transponder magnetic flux integration setup.

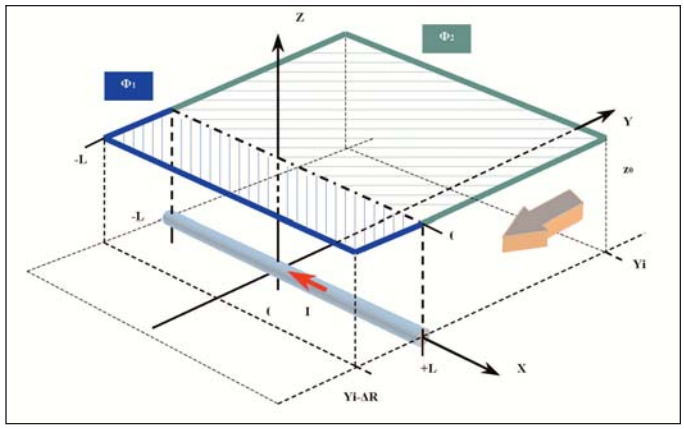

Figure 5 · Transponder crosswise movement—intersection.

Equation (16) was derived under an assumption that the magnetic flux created by a transponder itself has little effect on the magnetic field of the antenna.

The transponder magnetic flux for the interval where

$$\frac{\Delta R}{2} \le Y \le 0 \qquad (17)$$

was reconstructed from (16) representing the transponder by two parts (Fig. 5) having a total length ΔR with the limits for the first one Y_i–ΔR by ΔW and the second one $\boldsymbol{Y_i}$ by ΔW. By setting $R=0$ and making ΔR_i the variable in (16) the sum of the magnetic flux Φ_1 and Φ_2 on the interval (17) can be calculated considering their opposite directions.

Equation (16) for the magnetic flux through a transponder includes and relates the antenna length, distance to a transponder, its coil dimensions and the number of turns, and also indirectly considers an RF power available from the Reader by including the current I.

Antenna-Transponder Interaction

The proposed new antenna allows two alignments regarding transponder movement direction. These two movements named "Crosswise" and "Lateral" describe a transponder orientation in regards to an antenna plane. To facilitate an antenna-transponder interaction analysis and a performance comparison, the simple, but quite adequate for both cases, mathematical model described in (16) will be used.

To estimate an antenna SS for the transponder Crosswise movement (Fig. 4 and Fig. 6) the total transponder flux from an antenna carrying 80 mA current with 3 turns coil was calculated and plotted (Fig. 7) for the antenna location at $Y = 0$. There are four antennas having a length that ranges from 10 to 40 mm analyzed. The distance (the geometry mean distance) between an antenna wire and a transponder plane is $Z_0 = 5$ mm. The magnetic flux was calculated for the transponder 40 by 40 mm, which has 1 nWb the activation flux. For a 40 mm length antenna, the flux curve changes sharply, and for the second adjacent transponder the antenna has SS of approximately 8 dB, the interaction interval has two sep-

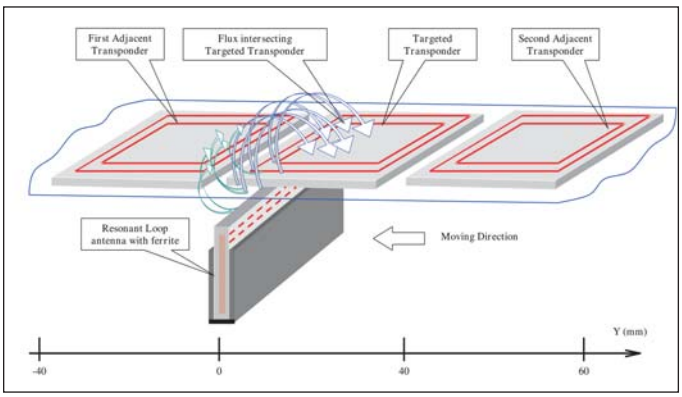

Figure 6 · Transponder crosswise movement.

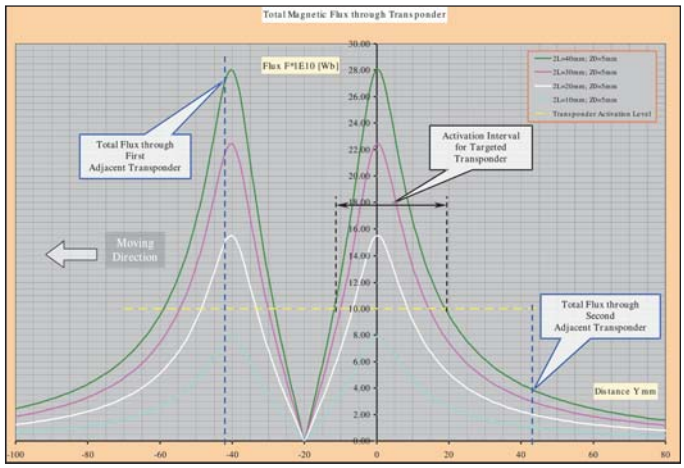

Figure 7 · Total magnetic flux through transponder for crosswise movement.

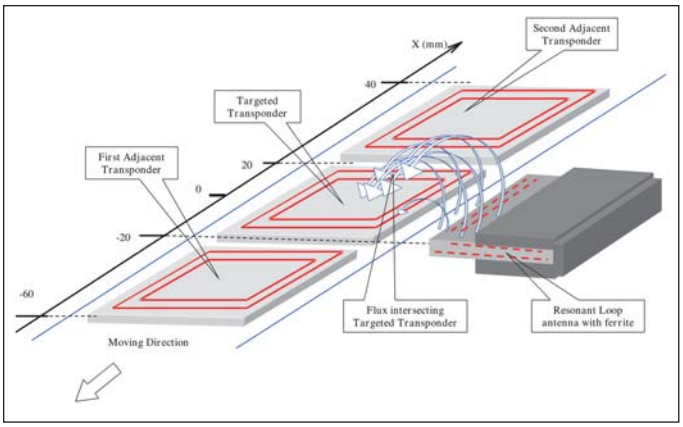

Figure 8 · Transponder lateral movement.

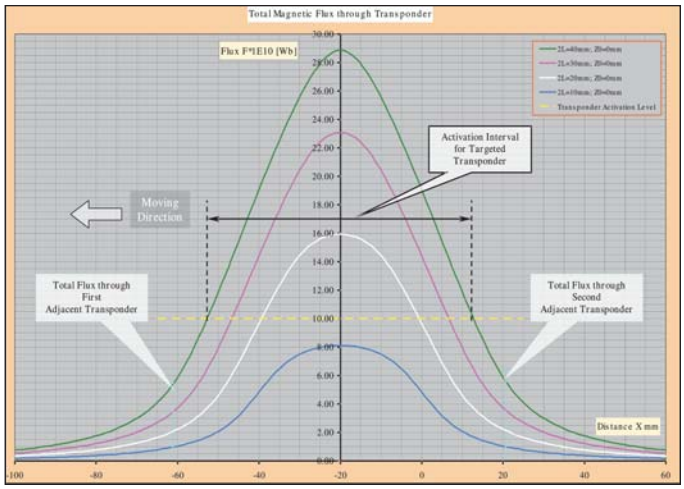

Figure 9 · Total magnetic flux through transponder for lateral movement.

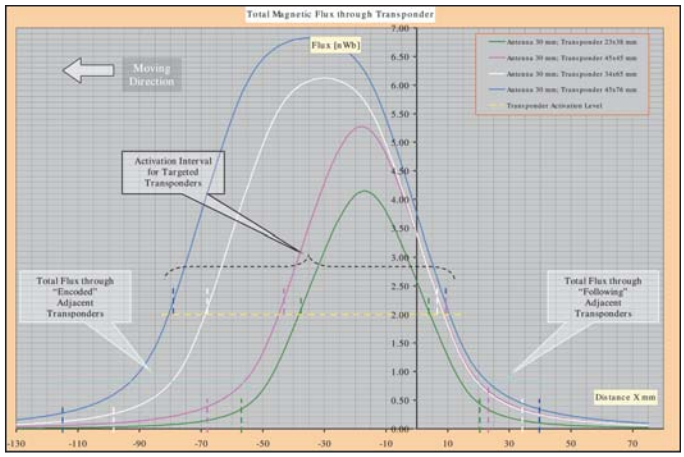

Figure 10 · Total magnetic flux through four transponders for lateral movement.

arated parts. For the Second Adjacent Transponder (Fig. 7) that is ~40 mm apart from the targeted transponder, SS of this antenna is negative (–8.5 dB). The total magnetic flux trough the transponder exceeds its activation level thus presenting a collision situation. While the activation interval for the targeted transponder is only 30 mm, the antenna for such alignment can be used successfully for a small item-level RFID only if the First Adjacent Transponder (Fig. 6 and 7) is moving out from a conveyor belt after being encoded.

For a transponder Lateral movement and corresponding alignment shown in Fig. 4 and Fig. 8, the curve of the total flux trough the transponder is not as sharp as for the previously considered alignment but instead there is the single, relatively wide, interaction interval (Fig. 9). The same four antennas with the length ranging from 10 to 40 mm were analyzed for the position co-centered at X = 0. The distance between the antenna wires and the transponder edge (the geometry mean distance) is R = 5 mm and the separation is Z_0 = 0. The magnetic flux was calculated for the similar transponder. For 40 mm antenna length, its SS is ~4.5 dB for both adjacent transponders and the activation interval for the targeted transponder is ~65 mm. The flux or power margin exceeds 9 dB, which makes an interrogation process very reliable. For the antennas centered at X = 0 with length decreasing from 40 to 30 and 20 mm the activation intervals shrink from 65 mm to 55 and 38 mm accordingly, and the relative activation flux or power changes proportionally from 9 dB to 7 and 4 dB. The antenna with 10 mm length is unable to activate the transponder. The biggest advantages of such alignment are the wide activation interval, high spatial selectivity and RF power margin.

Figure 10 depicts the total magnetic flux curves for four transponders (Lateral movement) spaced 5 mm apart from the antenna having 3 wires, 200 mA current and 30 mm length and centered at X = 0. With average transponder activation flux of approximately 2 nWb, the antenna demonstrates high spatial selectivity for all transponders in wide dimensional range (see Table 1). Maximum Relative Activation Flux was calculated for every transponder co-centered with the antenna.

Antenna Circuit

The magnetic flux produced by an antenna will intersect the wires in the transponder coil and create current flow. The induced current flow in the transponder will have its own magnetic flux, which will interact with the magnetic flux of an antenna. At some point, current induced in an antenna circuit by transponder flux can become comparable with an antenna current and, consequently, change its impedance and magnetic flux. Thus a current flowing in the antenna coil is defined by RF power from the Reader and an impedance that depends on properties of both magnetically coupled resonant circuits.

Transponder dimensions (mm)	SS for an "encoded" transponder (dB)	SS for a "following" transponder (dB)	Maximum Relative Activation Flux (dB)
23 × 38	15.4	12	6.3
45 × 45	14.2	8.9	8.4
34 × 65	17.4	15	9.7
45 × 76	16.8	14.7	10.6

Table 1 · Summary of SS and magnetic activation flux for four different transponder sizes.

To find a complete description of the current in an antenna coil it is necessary to know the parameters that characterize a relationship between the geometric structure of an antenna-transponder and their electrical components. The first parameter called the mutual inductance M relates two nearby coils of magnetically coupled devices. The mutual inductance depends on the geometrical arrangement of both circuits. The parameter M can be obtained from (16) and expressed as

$$\mathrm{M} = \frac{\Phi_T}{I}[\mathrm{H}] \tag{18}$$

Then impedance $\boldsymbol{Z_{AT}}$ induced in the antenna circuit by the transponder circuit [11] can be written as

$$Z_{AT} = \frac{(2\pi f \mathrm{M})^2 R_{TS}}{R_{TS}^2 + X_T^2} - j\frac{(2\pi f \mathrm{M})^2 X_T}{R_{TS}^2 + X_T^2} \tag{19}$$

where R_{TS} is equivalent resistive component of transponder impedance, and X_T is equivalent reactive component of transponder impedance.

If both antenna and transponder circuits are tuned at resonance with $X_T = 0$, Equation (19) becomes

$$R_{AT} = \frac{(2\pi f \mathrm{M})^2}{R_T}[\mathrm{ohm}] \tag{20}$$

where R_{AT} is a resistive component induced in an antenna by a transponder.

Thus antenna impedance at the resonance consists of its equivalent resistance R_{AL} associated with circuit losses in series with resistance R_{AT} (20).

The second parameter called the coupling coefficient K is the ratio showing a grade of coupling between two devices and defined as

$$K = \frac{\mathrm{M}}{\sqrt{L_A L_T}} \tag{21}$$

where L_A is the apparent inductance of an antenna coil, and L_T is the inductance of a transponder coil.

The magnetic flux through a transponder coil is increasing when it comes close to an antenna and so does the coupling coefficient. At some separation distance an antenna-transponder coupling attains critical level at which power transfer efficiency from antenna to transponder achieves its maximum and R_{AL} becomes equal to R_{AT}. Then the third parameter called the critical coupling coefficient K_c linking Q-factors of both circuits for this case

$$K_c = \frac{1}{\sqrt{Q_A Q_T}} \tag{22}$$

As required for the critical coupling, an apparent inductance L_A of an antenna coil can be obtained by combining (18), (21) and (22)

$$L_A = \frac{\Phi_T}{I\sqrt{\frac{L_T^2}{Q_A Q_T}}}$$

In order to maintain the same transponder magnetic flux for the critical coupling as for the loosely coupled case, RF power from a Reader must be doubled and antenna impedance matched to $2R_{AL}$.

Matching an antenna combined impedance when the critical coupling takes place for a transponder positioned at the center of an activation interval further increases an antenna SS. Improved SS is achieved because the transponder movement to any of two positions corresponding to the edges of the activation interval causes an antenna impedance mismatch. The impedance mismatch in turn decreases the power transfer efficiency and as a result lowers the magnetic flux available for two adjacent transponders. If a design goal is to enlarge an activation interval then an adaptive impedance matching might be implemented. The antenna impedance adaptive matching uses adjustable matching components, which parameters changes depending on an antenna coupling grade with a transponder to keep antenna port impedance equal to an impedance of RF power source.

The antenna coil practical design presented here is a multi-interactive process, but regardless of the type of a fabrication technology, an apparent inductance can be measured and confirmed after covering three sides of a rectangular coil by the flexible ferrite with permeability in the range of 20 to 40 [12, 13]. Utilization of ferrite materials with higher permeability is limited by the minimum value of antenna resonating capacitive elements, which should be no less than 50 pF to prevent circuit detuning in the operating environment.

Conclusions

A single element antenna allows for precise identification of closely spaced miniature objects with a wide range of transponder geometries. This spatially selective antenna, and the mathematical model developed for its analysis, are not restricted in size and may be successfully applied to widespread RFID applications involving large-scale structures.

One limitation of a highly spatially selective antenna is that, despite its proximity to the transponder, the antenna requires the same RF power as a conventional antenna for long range RFID applications. This limitation applies only to HF transponders activated by the antenna's magnetic field, whereas battery powered transponders require significantly less power for the antenna. For conveyor-type RFID applications in crowded environments with surrounding metal and plastic parts, the magnetic field becomes distorted. Such environments can increase power losses, detune both the antenna and the transponder, and require higher power for transponder activation compared to open environments. Nonetheless, the antenna-transponder coupling was analyzed and a working system implemented for the HF RFID printer-encoders using the mathematical model described in this article. Empirically obtained corrective coefficients for transponder activation power, power margin and relative activation power have shown encouraging results.

A complete analytical model for magnetic flux analysis in crowded environments, and antenna-transponder coupling may be further explored using HF structure simulator software. This model should also take into consideration the current increase in a transponder coil when the magnetic field exceeds transponder activation flux and the IC voltage regulator is engaged.

Acknowledgements

The author would like to thank Dr. Hohberger, C.P., Torchalski, K.,

and Schwan, M., at Zebra Technologies Corporation for helpful and productive discussions regarding HF RFID spatially selective antennas development and Gawelczyk, R., for his assistance in antennas fabrication and testing.

Appendix

An Appendix that includes the derivation of Equation 16 is included with the online version of this article at www.highfrequencyelectronics.com.

References

1. P. Albert, D. Ruffieux, O. Zhuk, "Understanding the Role of NFC-Based RFID Devices in the Consumer/Mobile Market," Emerging Wireless Technology/A Supplement to *RF Design,* pp. 2-4, August, 2005.

2. "Find a Vendor," *RFID Journal,* 2006. http://www.rfidjournal.com/article/findvendor.

3. K. Finkenzeller, *RFID Handbook-Fundamentals and Applications in Contactless Smart Cards and Identification,* Second Edition, John Wiley & Sons, 2003. ISBN: 0-470-84402-7.

4. Y. Lee, "Antenna Circuit Design for RFID Applications," AN710, Microchip Technology Inc., 2003. http://ww1.microchip.com/downloads/en/appnotes/00710c.pdf.

5. "Tutorial Overview of Inductively Coupled RFID Systems," UPM Rafsec, May 2003. http://www.rafsec.com/rfidsystems.pdf.

6. "Tag-it HF-I Standard Transponder Inlays," Reference Guide. Lit number: 11-09-21-062, Texas Instruments Incorporated, Dec. 2005. http://www.ti.com/rfid/docs/manuals/refmanuals/HF-IStandardInlays-RefGuide.pdf.

7. "HF tags and inlays, standard products," UPM Raflatac, 2006. http://www.rafsec.com/hf_availability.htm.

8. G. Zhong, C-K. Koh, "Exact Closed Form Formula for Partial Mutual Inductances of On-Chip Interconnects," *IEEE 20th International Conference on Computer Design*, Freiburg, Germany, 2002. http://www.iccd-conference.org/proceedings/2002/17000428.pdf.

9. B.Y. Tsirline, C.P. Hohberger, R. Gawelczyk, "System and Method for Selective Communication with RFID Transponders," U.S. Patent 6,848,616, B2, February 2005.

10. M.I. Grivich, D.P. Jackson, "The magnetic field of current-carrying polygons: An application of vector field rotations," American Association of Physics Teachers, *American Journal of Physics,* Vol. 68, No. 5, pp. 469-474, May 2000. http://physics.dickinson.edu/~dept_web/activities/papers/polygonarticle.pdf.

11. D.A. Bell, *Fundamentals of Electric Circuits / With Computer Program Manual,* 4th Edition, Prentice Hall, 1988. ISBN: 0-13-336645-6.

12. "RFID Absorber Shielding," FerriShield, Inc., 2006. http://www.ferrishield.com.

13. "Flex-Suppressor," NEC TOKIN America Inc., Vol.08, 2006. http://www.nec-tokin.com/english/product/pdf_dl/FLEX.pdf.

14. K. Gieck, R. Gieck, *Engineering Formulas,* 6th edition, McGraw-Hill Inc., 1990. ISBN: 0-07-023455-8.

Author Information

Boris Y. Tsirline is the senior RFID research engineer at Zebra Technologies Corporation in Vernon Hills, IL. He received a BS and MS degrees in RF & Microwave Engineering from Moscow Aviation University, Russia in 1973 and a PhD in EE from Moscow State University in 1986. Before moving to the US in 1992, he served as a Director of R&D at Automotive Electronics and Equipment Corp., Russia, developing military and aerospace electronic systems. He has been in the Automatic Identification and Data Capture industry since 1995; first as an RF Engineer involved in LF RFID design of automotive immobilizers at TRW (Automotive Electronic Group) and then at Zebra Technologies Corporation since 1998. He managed the development of Zebra's first HF RFID printer-encoder and established the design methodology for HF and UHF spatially selective antenna-transponder structures used throughout the corporation divisions for RFID labels and cards printers. Dr. Tsirline holds three non-classified Russian and two US patents and has numerous pending patents for RFID enhancements.

Appendix

$$\Phi_T = \frac{\mu_0 NI}{4\pi} \int_R^{R+\Delta R} \frac{ydy}{\left(y^2 + z_0{}^2\right)} \int_W^{W+\Delta W} \frac{(x+L)\,dx}{\sqrt{(x+L)^2 + \left(y^2 + z_0{}^2\right)}} - \int_R^{R+\Delta R} \frac{ydy}{\left(y^2 + z_0{}^2\right)} \int_W^{W+\Delta W} \frac{(x+L)\,dx}{\sqrt{(x-L)^2 + \left(y^2 + z_0{}^2\right)}} \tag{1}$$

$$\int_W^{W+\Delta W} \frac{(x+L)\,dx}{\sqrt{(x+L)^2 + \left(y^2 + z_0{}^2\right)}} \tag{2}$$

To do this integral we'll use the following substitution: $x + L = \rho$ and $y_2 + z_0{}^2 = \varepsilon^2$

then $d\rho = dx$ and an integral from formula "i88" [14]

$$\int \frac{\rho}{\sqrt{\left(\rho^2 + \varepsilon^2\right)}} d\rho = \sqrt{\rho^2 + \varepsilon^2} \tag{3}$$

Integral (2) can be written as:

$$\sqrt{\left(y^2 + z_0{}^2\right) + (x+L)^2}\Big|_W^{W+\Delta W} = \sqrt{\left(y^2 + z_0{}^2\right) + (W + \Delta W + L)^2} - \sqrt{\left(y^2 + z_0{}^2\right) + (W+L)^2} \tag{4}$$

or equation (4) can be presented in a form of

$$= \sqrt{y^2 + \left[z_0{}^2 + (W + \Delta W + L)^2\right]} - \sqrt{y^2 + \left[z_0{}^2 + (W+L)^2\right]} \tag{5}$$

substituting first component in (1)

$$\int_R^{R+\Delta R} \left(\frac{y\sqrt{y^2 + \left[z_0{}^2 + (W + \Delta W + L)^2\right]}}{\left(y^2 + z_0{}^2\right)} - \frac{y\sqrt{y^2 + \left[z_0{}^2 + (W+L)^2\right]}}{\left(y^2 + z_0{}^2\right)} \right) dy \tag{6}$$

To do integral (6) we'll use the following substitution for the first component:

$$\lambda = \sqrt{y^2 + \left[z_0{}^2 + (W + \Delta W + L)^2\right]}$$

then

$$\lambda^2 = y^2 + \left[z_0{}^2 + (W + \Delta W + L)^2\right]$$

$$y^2 = \lambda^2 - \left[z_0{}^2 + (W + \Delta W + L)\right.$$

and

$$y = \sqrt{\lambda^2 - \left[z_0{}^2 + (W + \Delta W + L)^2 \right]}$$

then

$$dy = \frac{\lambda}{\sqrt{\lambda^2 - \left[z_0{}^2 + (W + \Delta W + L)^2 \right]}} d\lambda$$

and use the following substitution for the second component:

$$\sigma = \sqrt{y^2 + \left[z_0{}^2 + (W + L)^2 \right]}$$

then

$$\sigma^2 = y^2 + \left[z_0{}^2 + (W + L)^2 \right]$$

$$y^2 = \sigma^2 - \left[z_0{}^2 + (W + L)^2 \right]$$

and

$$y = \sqrt{\sigma^2 - \left[z_0{}^2 + (W + L)^2 \right]}$$

then

$$dy = \frac{\sigma}{\sqrt{\sigma^2 - \left[z_0{}^2 + (W + L)^2 \right]}} d\sigma$$

Integral (6) can be written as:

$$\int_R^{R+\Delta R} \frac{\lambda^2}{\lambda^2 - (W + \Delta W + L)^2} d\lambda - \int_R^{R+\Delta R} \frac{\sigma^2}{\sigma^2 - (W + L)^2} d\sigma$$

substituting $(W + \Delta W + L)^2 = \xi^2$ and $(W + L)^2 = a^2$

$$\int \frac{\lambda^2}{\lambda^2 - \xi^2} d\lambda = \lambda - \frac{\lambda}{2} Ln \left| \frac{\xi + \lambda}{\xi - \lambda} \right|$$

and

$$\int \frac{\sigma^2}{\sigma^2 - a^2} d\sigma = \sigma - \frac{a}{2} Ln \left| \frac{a + \sigma}{a - \sigma} \right| \qquad \text{[formula “i61” 14,]}$$

Then two components of integral (6) can be rewritten as

$$\sqrt{y^2 + \left[z_0{}^2 + (W + \Delta W + L)^2 \right]} \Bigg|_R^{R+\Delta R} - \frac{(W + \Delta W + L)}{2} Ln \left| \frac{(W + \Delta W + L) + \sqrt{y^2 + z_0{}^2 + (W + \Delta W + L)^2}}{(W + \Delta W + L) - \sqrt{y^2 + z_0{}^2 + (W + \Delta W + L)^2}} \right| \Bigg|_R^{R+\Delta R} \tag{7}$$

and

$$\sqrt{y^2 + \left[z_0{}^2 + (W + L)^2 \right]} \Bigg|_R^{R+\Delta R} - \frac{(W + L)}{2} Ln \left| \frac{(W + L) + \sqrt{y^2 + z_0{}^2 + (W + L)^2}}{(W + L) - \sqrt{y^2 + z_0{}^2 + (W + L)^2}} \right| \Bigg|_R^{R+\Delta R} \tag{8}$$

using (7) and (8) integral (6) is then

$$\sqrt{(R+\Delta R)^2+z_0{}^2+(W+\Delta W+L)^2}-\sqrt{(R)^2+z_0{}^2+(W+\Delta W+L)^2}-$$

$$-\frac{(W+\Delta W+L)}{2}Ln\left|\frac{(W+\Delta W+L)+\sqrt{(R+\Delta R)^2+z_0{}^2+(W+\Delta W+L)^2}}{(W+\Delta W+L)-\sqrt{(R+\Delta R)^2+z_0{}^2+(W+\Delta W+L)^2}}\right|$$

$$+\frac{(W+\Delta W+L)}{2}Ln\left|\frac{(W+\Delta W+L)+\sqrt{R^2+z_0{}^2+(W+\Delta W+L)^2}}{(W+\Delta W+L)-\sqrt{R^2+z_0{}^2+(W+\Delta W+L)^2}}\right|-$$

$$-\sqrt{(R+\Delta R)^2+z_0{}^2+(W+L)^2}+\sqrt{(R)^2+z_0{}^2+(W+L)^2}+$$

$$+\frac{(W+L)}{2}Ln\left|\frac{(W+L)+\sqrt{(R+\Delta R)^2+z_0{}^2+(W+L)^2}}{(W+L)-\sqrt{(R+\Delta R)^2+z_0{}^2+(W+L)^2}}\right|-$$

$$-\frac{(W+L)}{2}Ln\left|\frac{(W+L)+\sqrt{R^2+z_0{}^2+(W+L)^2}}{(W+L)-\sqrt{R^2+z_0{}^2+(W+L)^2}}\right| \qquad (9)$$

By repeating procedure above for:

$$-\int_{W}^{W+\Delta W}\frac{(x-L)\,dx}{\sqrt{(x-L)^2+\left(y^2+z_0{}^2\right)}}$$

and substituting a second component in (1)

$$-\int_{R}^{R+\Delta R}\frac{\gamma^2}{\gamma^2-(W+\Delta W-L)^2}\,d\gamma+\int_{R}^{R+\Delta R}\frac{\nu^2}{\nu^2-(W-L)^2}\,d\nu$$

where

$$\gamma=\sqrt{y^2+\left[z_0{}^2+(W-L)^2\right]}$$

and

$$\nu=\sqrt{y^2+\left[z_0{}^2+(W-L)^2\right]}$$

we can compute

$$-\sqrt{(R+\Delta R)^2+z_0^{\,2}+(W+\Delta W-L)^2}+\sqrt{(R)^2+z_0^{\,2}+(W+\Delta W-L)^2}+$$

$$+\frac{(W+\Delta W-L)}{2}Ln\left|\frac{(W+\Delta W-L)+\sqrt{(R+\Delta R)^2+z_0^{\,2}+(W+\Delta W-L)^2}}{(W+\Delta W-L)-\sqrt{(R+\Delta R)^2+z_0^{\,2}+(W+\Delta W-L)^2}}\right|-$$

$$-\frac{(W+\Delta W-L)}{2}Ln\left|\frac{(W+\Delta W-L)+\sqrt{R^2+z_0^{\,2}+(W+\Delta W-L)^2}}{(W+\Delta W-L)-\sqrt{R^2+z_0^{\,2}+(W+\Delta W-L)^2}}\right|+$$

$$+\sqrt{(R+\Delta R)^2+z_0^{\,2}+(W-L)^2}+\sqrt{(R)^2+z_0^{\,2}+(W-L)^2}-$$

$$-\frac{(W-L)}{2}Ln\left|\frac{(W-L)+\sqrt{(R+\Delta R)^2+z_0^{\,2}+(W-L)^2}}{(W-L)-\sqrt{(R+\Delta R)^2+z_0^{\,2}+(W-L)^2}}\right|+$$

$$+\frac{(W-L)}{2}Ln\left|\frac{(W-L)+\sqrt{R^2+z_0^{\,2}+(W-L)^2}}{(W+L)-\sqrt{R^2+z_0^{\,2}+(W-L)^2}}\right| \qquad (10)$$

Adding (9) and (10), we will obtain a final result (Equation 16).